Disentangling local heat contributions in interacting magnetic nanoparticles

C. Muñoz-Menendez,[1] D. Serantes [ORCID],[1] O. Chubykalo-Fesenko [ORCID],[2,*] S. Ruta,[3] O. Hovorka,[4] P. Nieves,[5] K. L. Livesey,[6,7]
D. Baldomir,[1] and R. Chantrell [ORCID][3]

[1]*Instituto de Investigacións Tecnolóxicas and Departamento de Física Aplicada, Universidade de Santiago de Compostela,*
15782 Santiago de Compostela, Spain

[2]*Instituto de Ciencia de Materiales de Madrid, CSIC, Cantoblanco, ES-28049 Madrid, Spain*

[3]*Department of Physics, University of York, York YO10 5DD, England, United Kingdom*

[4]*Faculty of Engineering and the Environment, University of Southampton, Highfield, Southampton, England, United Kingdom*

[5]*IT4Innovations, VŠB – Technical University of Ostrava, Listopadu 2172/15, 70800 Ostrava-Poruba, Czech Republic*

[6]*Biofrontiers Center and Department of Physics, University of Colorado Colorado Springs, Colorado Springs, Colorado 80918, USA*

[7]*The University of Newcastle, Callaghan NSW 2308, Australia*

Recent experiments on magnetic nanoparticle hyperthermia show that the heat dissipated by particles must be considered locally instead of characterizing it as a global quantity. Here we show theoretically that the complex energy transfer between nanoparticles interacting via magnetic dipolar fields can lead to negative local hysteresis loops and does not allow the use of these *local* hysteresis loops as a temperature measure. Our model shows that interacting nanoparticles release heat not only when the nanoparticle magnetization switches between different energy wells, but also in the intrawell motion, when the effective magnetic field is changed because the magnetization of another particle has switched. The temperature dynamics has a highly nontrivial dependence on the amount of precession, which is controlled by the magnetic damping. Our results constitute a step forward in modeling magnetic nanoparticles for hyperthermia and other heating applications.

I. INTRODUCTION

The ability of magnetic nanoparticles to release heat under varying external electromagnetic fields finds important applications in chemical catalysis [1], the automotive and aeronautical industries [2], and biomedicine [3]. One of the most important examples is magnetic nanoparticle hyperthermia (MNH)—a promising technique for cancer treatment whereby tumors are heated a few degrees Celsius to cause cell death. While MNH has reached clinical application [4], it has not attained its anticipated full potential as a complement/alternative to standard therapies [5]. A major contributing factor to the slow advances in MNH is the lack of understanding of the physical processes underlying the heating mechanism.

Typically, the efficiency of nanoparticle systems for MNH is characterized by measurement of the specific absorption rate (SAR), which is related to the global increase of temperature over many cycles of the alternating field. On the other hand, several experiments [6–8] stress the importance of local heat release around the nanoparticle. It was shown, for example, that the temperature rapidly decreases in less than 10 nm from the nanoparticle surface [7], as illustrated in Fig. 1. In other words, the local temperature around a nanoparticle is different from that of the surrounded media and may be more important for understanding the MNH efficiency than global

heating. Moreover, recent experiments [9,10] demonstrate that effective MNH therapy is possible *in the absence of a global rise in temperature*. This clearly demonstrates the necessity to understand heat as a spatially dependent quantity.

In addition, interactions between particles must be considered for the reasons described below. Firstly, substantial differences between *in vivo* and *in vitro* heating properties are reported in the literature [11,12]. One of the important reasons for this is that within a tumor magnetic nanoparticles can form aggregated (strongly interacting) fractal structures [13], whereas in the laboratory they are in well-dispersed stable fluid suspensions. Secondly, the intricately entwined effects of particle properties and experimental protocols on MNH heating (even for homogeneously distributed samples) become further complex when aggregation occurs. In fact, depending on conditions, interactions have been reported to be both beneficial and detrimental to MNH [14].

Experimental evaluation of magnetic hyperthermia performance is based on the SAR measurement on an ensemble of nanoparticles. In modeling, the released heat is typically evaluated as proportional to the hysteresis loop area [15]. A range of different approaches have been used to evaluate the hysteresis loops of ensembles, including kinetic Monte Carlo techniques [16,17] and an equivalent master equation model [18,19], which are suitable for the typical timescales of magnetic hyperthermia experiments (tens to hundreds of kilohertz). These approaches require an evaluation of reversal probabilities to traverse over energy barriers, which is not a trivial task in the presence of magnetic interactions,
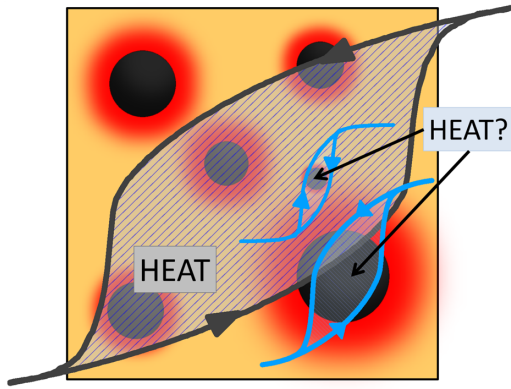
*oksana@icmm.csic.es

FIG. 1. Illustration of *global vs local* heat in a nanoparticle ensemble: do individual (single-particle) loops represent local heating?

even between just two particles [20], and involves various approximations [21]. While the mentioned calculations are very useful to evaluate magnetic relaxation of an *ensemble* of nanoparticles, they are intrinsically statistical approaches dealing with distribution functions and do not aim to find local temperature changes. In this article we instead find the local heat dynamics around *individual* nanoparticles and use an entirely different approach that is inspired by recent experiments [6–8] that indicate the importance of this heat dynamics for cancer treatment. We also point to the influence of interactions on not just *where* the heating occurs in a system of multiple particles but also on the temperature dynamics (i.e., how local temperature evolves in time), an aspect which was not discussed in the literature until now.

Given the above fact that the local heating might be more important than the global temperature rise, the following question is posed: How can one calculate the local heat produced by individual particles in the case of interacting systems? Classical thermodynamics for an isolated system states that the released heat is proportional to the hysteresis loop area (work) for a cyclic magnetic process. Thus one could be tempted to directly consider the loop area of each interacting nanoparticle and relate this to a local temperature rise [16,22]. This approach, however, is not correct due to the fact that an

individual nanoparticle does not form an isolated system and does work on its interacting counterpart. Our recent consideration of the thermodynamics of interacting nanoparticles [19] showed that also within a statistical approach—rather than a dynamical approach as described here—one cannot evaluate released heat from individual particle hysteresis loops and an explicit evaluation of entropy production is necessary.

In this work we present a model approach based on the self-consistent treatment of magnetization and temperature dynamics [23] which allows one to estimate local heating in an interacting magnetic nanoparticle system. Our results allow us to discuss the conditions for heat release by individual nanoparticles. Particularly, we show that interacting nanoparticles may dissipate significant heat not only during their interwell magnetization switching (flipping from one direction to another) but also during intrawell dynamics when a neighboring particle undergoes switching. The total dissipated heat (plus the time the heat takes to dissipate from the magnetic degrees of freedom) in these processes depends on the damping constant, as this controls the amount of precession. It is well known that work and heat are path-dependent thermodynamic quantities, and so changes in the degree of precession change the heating. What is more dramatic is that the distribution of the heat between different particles is changed strongly by varying the damping.

II. MODEL AND RESULTS

Our trial example is the simplest one of two immobilized nanoparticles, as then heat is not produced via Brownian translations or rotations but only through internal magnetization dynamics. The nanoparticles' switching fields are deliberately made to be different in order to separate the switching events in time. Namely, we consider two particles, A with diameter $D = 22$ nm and easy axis parallel to the applied field direction, and B with $D = 18$ nm, easy axis directed at $30°$ to the field direction. See cartoon balls in Fig. 2, where A is in red and B is in blue. Both particles have the same uniaxial anisotropy constant $K = 10^5$ erg/cm^3 and saturation magnetization $M_S = 480$ emu/cm^3. The magnetic field has the oscillatory form $h = h_{max} \cos(2\pi f t)$, where t is time.
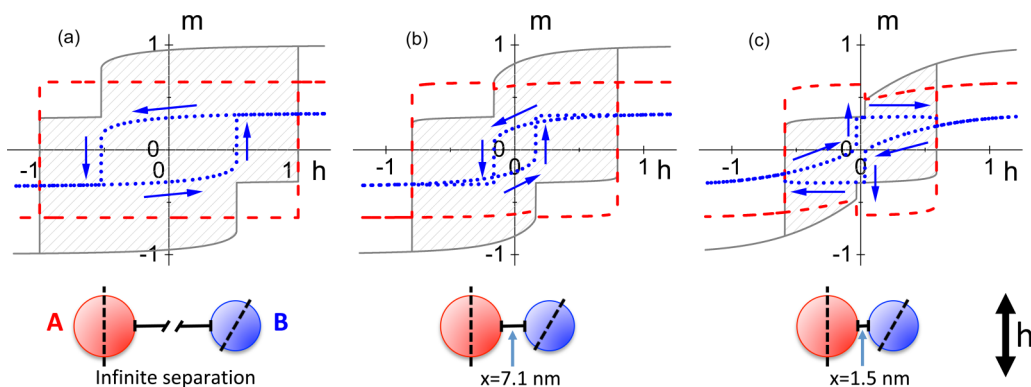

FIG. 2. Global (dashed area) and local (red for large particle A and blue for small particle B) hysteresis cycles for two interacting nanoparticles, separated by different distances x along the perpendicular to the field direction. Cases are (a) noninteracting, (b) $x = 7.1$-nm separation, and (c) 1.5-nm separation. Schematics of the two particles are drawn below each set of cycles, with their anisotropy axes drawn by dashed lines.

We use $h_{max} = 500$ Oe and $f = 500$ kHz. These parameters correspond to Fe_3O_4 particles and external field conditions commonly used in MNH experiments. The nanoparticles' centers are in the plane formed by the applied field and easy axes. The particles have a surface-to-surface separation x along the line perpendicular to the external field. The nanoparticles interact via dipole-dipole interactions, with each particle approximated as having a single magnetic moment.

The *local* (individual particle) and *global* (system average) hysteresis loops of nanoparticles at 0 K and with infinitely slow field variation can be calculated by a direct energy-minimization technique. The results are presented in Fig. 2 for three values of separation distance x. The area of the global hysteresis loops (shaded regions) corresponds to the released heat and is seen to decrease when the separation distance decreases. The area of local loops (corresponding to the magnetization change of each nanoparticle, red and blue loops) also decreases. Furthermore, the smallest considered interparticle distance [Fig. 2(c) with $x = 1.5$ nm] produces a so-called "inverted loop" for the smaller nanoparticle B. A small part of B's loop is also inverted in Fig. 2(b) with $x = 7.1$ nm in the first and third quarters of the hysteresis loop. Such inverted loops have been measured experimentally in ensembles of interacting superparamagnetic and blocked nanoparticles and are typically attributed to the role of magnetic interactions [24,25]. The immediate question arises: How do we interpret the local inverted loops? The naive interpretation would be that the nanoparticle cools the environment instead of heating it. Note that since the calculations are done at zero Kelvin, this is thermodynamically impossible and so this naive interpretation is incorrect. In fact, work is being done on the particle by the dipolar interaction with the other particle, in addition to the heat transfer to the environment.

Before describing how to correctly find the heat released by the individual particles, we examine the magnetization reversal processes of the two-particle system. Figure 3 presents the evolution of (a) the magnetization and (b) the energy of each nanoparticle corresponding to the case of $x = 7.1$ nm separation, i.e., to Fig. 2(b), calculated either using energy minimization or a dynamical approach [integration of the Landau-Lifshitz-Gilbert (LLG) equation with high damping value]. Since the timescale of the field change is much slower than that of the nanoparticle switching, the two approaches give identical results. However, the dynamical approach allows one to calculate corresponding changes in temperature [23] (see Fig. 3(c), which will be discussed later), whereas we found that energy minimization cannot do so. It is worth mentioning that while for the direct comparison with the energy-minimization approach it was desirable to have negligible thermal effects, we found that finite-temperature calculations produce essentially the same features just with more noise.

One can distinguish two magnetization variations in Fig. 3: first, the magnetization of both particles can vary continuously, such as from $t = 0$ to $t = 0.55\,\mu$s, in a so-called reversible change. It corresponds to work being done by the changing external field to increase the energy of the system up to the point of the irreversible transition. Second, an *irreversible* magnetization variation occurs where there is an abrupt change (*jump*) in both particles' magnetization and
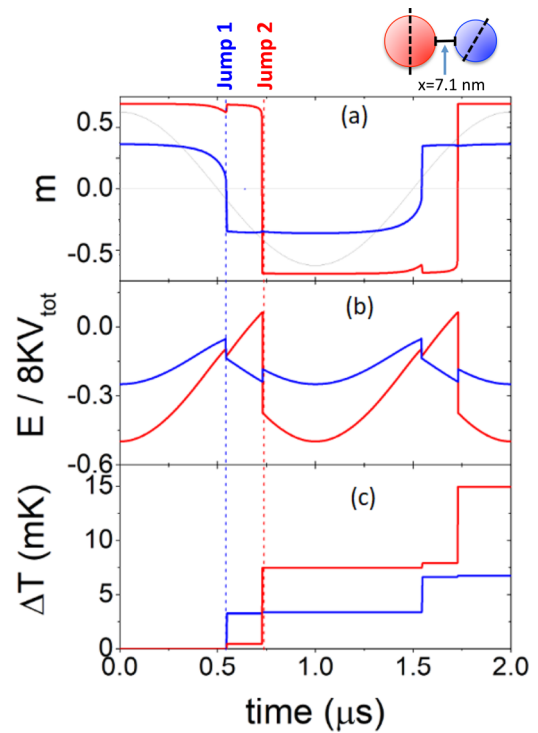

FIG. 3. Dynamics of (a) normalized magnetization, (b) total energy (normalized by the maximum possible stored energy $2M_s 2H_K V_{tot} = 8KV_{tot}$, where V_{tot} is the system volume and $H_K = 2K/M_s$ is the anisotropy field), and (c) temperature change ΔT as computed by Eq. (1). The blue line corresponds to nanoparticle B and the red line to nanoparticle A. The nanoparticles are separated by $x = 7.1$ nm.

total magnetic energy. At each jump, two types of processes can be distinguished, which we will call interwell and intrawell processes. An interwell process corresponds to a particle's magnetic moment switching direction from one energy minimum to the other. Namely, the switching of small nanoparticle B [jump 1 at $t = 0.55\,\mu$s, blue curve in Fig. 3(a)] and then the switching of large nanoparticle A [jump 2 at $t = 0.75\,\mu$s, red]. Simultaneous with these interwell processes are intrawell processes by the other, "nonswitching" nanoparticles. The magnetization changes are much smaller as the particle stays in the same local energy well. For example, at $t = 0.55\,\mu$s (jump 1), the magnetization of A actually increases slightly in magnitude, in a direction opposite to the applied magnetic field, due to B switching.

The particles are obviously doing work on each other, and for this reason their individual hysteresis loops cannot be used to estimate the heat that each produces. Note that *only* in the case of noninteracting nanoparticles [Fig. 2(a)] can individual hysteresis loops be used to compute the heat released by each nanoparticle and the global heat released, as then there is just one interaction with the external field.

If hysteresis loops cannot be used to estimate the heat produced by A and that produced by B when the particles interact, then another calculation method is needed. We use a recently derived self-consistent framework for magnetization dynamics in contact with a heat bath [23]. Disregarding the self-heating of nanoparticles (the change of the

magnetization's magnitude, which is negligible at low temperatures), the two coupled equations (written for each nanoparticle, so four equations in total) read

$$\frac{d\mathbf{m}}{dt} = -\gamma \mathbf{m} \times \mathbf{H}_{\text{eff}} - \gamma \alpha_\perp \mathbf{m} \times (\mathbf{m} \times \mathbf{H}_{\text{eff}}), \quad (1a)$$

$$\frac{dT_b}{dt} = \frac{\gamma \alpha_\perp M_s}{C_b}(\mathbf{m} \times \mathbf{H}_{\text{eff}})^2. \quad (1b)$$

Here $\mathbf{m} = \mathbf{M}/M_s$ ($T = 0$ K) is the reduced magnetization vector, $\mathbf{H}_{\text{eff}}$ is the total internal field comprised of the anisotropy, Zeeman, and dipolar contributions, γ is the gyromagnetic factor, T_b is the *local* temperature of the particle, $C_b = 3.48 \times 10^6$ J m^{-3} K^{-1} is the specific heat capacity of magnetite, and $\alpha_\perp$ is the damping parameter. In this simplified case, the first Eq. (1a) is just the micromagnetic LLG equation and the second Eq. (1b) is similar to that which is derived from the Rayleigh function (up to the $\alpha_\perp^2$ terms). The latter approach was used, for example, in Refs. [26,27].

Equation (1) clearly shows that the temperature change occurs for processes in which the magnetization is not parallel to the internal field $\mathbf{H}_{\text{eff}}$. This happens during the interwell dynamics, when the magnetization vector switches from one energy minimum to another, and also during intrawell (nonswitching) processes, since the interaction field changes when the magnetization of the other particle switches. The heat released in both cases will depend on the damping constant, as it affects the magnetization path. Both the amplitude and duration of the induced magnetization precession is altered by $\alpha_\perp$. The key point is that a particle can dissipate heat without switching its magnetization. Furthermore, whether the particle's magnetic energy increases or decreases is irrelevant as magnetization dynamics is occurring, work is being done, and therefore heat will be released. We remark that the heat dissipation occurs on the timescale of the magnetization dynamics (field-driven *switching* in nanoseconds), but the actual heat retained in the system will depend on the timescale of the consequent cooling [23].

To understand the energy change and heat dissipated of each nanoparticle during the hysteresis cycles presented in Fig. 2, we first use large damping parameter $\alpha_\perp = 1.0$. This removes most of the precession from the magnetization paths and makes the dynamical hysteresis loops very close to those obtained by energy minimization. Note that we found it impossible to completely remove the effect of precession in dynamical simulations. We checked that local hysteresis loops and the dynamical approach give the same temperature increase for the noninteracting case. Then we considered interactions. Figure 3(c) presents the temperature dynamics during the hysteresis cycle for interacting nanoparticles separated by $x = 7.1$ nm. The temperature increases for both particles at every jump, emphasizing that inverted loops do not correspond to energy absorption, as discussed earlier.

Figure 4 compares the internal energy change (obtained by energy minimization, solid bars) and the released heat [obtained by dynamical method Eq. (1), hashed bars] for each particle A (red) and B (blue). One can see from hysteresis loops that nanoparticle B (small) experiences an energy decrease during the switching of nanoparticle A (jump 2, solid blue bar). As mentioned earlier, one might interpret this as "cooling" if one were to ignore the work that the particles do
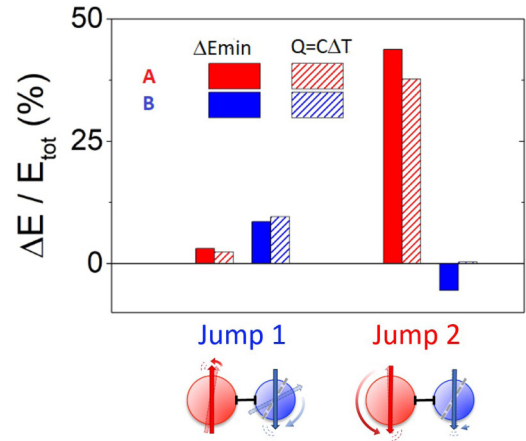

FIG. 4. A comparison of energy change (work plus heat, solid bars) and heat released (hashed bars) during the two irreversible magnetization jumps for the two particles A (red) and B (blue). The energy changes ΔE_{min} are evaluated from individual hysteresis loops, while the heat released Q is calculated using Eq. (1) with large damping $\alpha_\perp = 1.0$. The results are normalized to the total energy "stored" in the global hysteresis loop. The nanoparticles are separated by 7.1 nm, as in Fig. 3. The sketches illustrate whether the magnetization of the particle switches, or wobbles, within the same energy well.

on each other; however the dynamical approach shows that heat is produced by the particle and its temperature goes up.

The simulations above were done for a large damping parameter ($\alpha_\perp = 1.0$), which assured a better comparison and interpretation in terms of energy/work/heat, since the static and dynamical loops are practically the same. However, smaller damping parameters are more realistic for nanoparticles [28]. Figure 5 includes the results of varying $\alpha_\perp$ in the interval from 0.001 to 1. The temperature increase as a function of time in Fig. 5(a) shows slower heating as $\alpha_\perp$ decreases, with a very nonlinear behavior of the total dissipated heat. In Fig. 5(b), the temperature increase ΔT is plotted as a function of $\alpha_\perp$ for both particles at jump 1. In jump 1, nanoparticle B (blue, open circles) switches while A (open, red squares) does not. The temperature increases are almost independent of the damping parameter in the interval $\alpha_\perp \in (0.001, 0.2)$. Compared to the large damping case, for smaller damping the temperature increase is slightly smaller for nanoparticle B (switching) and slightly larger for nanoparticle A (nonswitching) for jump 1. This effect is due to the precession. In fact, both nanoparticles are precessing around their internal effective fields, which are also dynamically changing. Thus the switching particle B exerts an additional damping to the nonswitching particle A.

In Fig. 5(c), ΔT is plotted for both particles during jump 2 as a function of damping. The roles of the nanoparticles are interchanged compared to jump 1: now particle A (solid, red squares) switches its magnetization.

In the limit of large damping, particle B has negligible temperature increase, indicating that the work done on it all goes to increasing the internal energy. But the temperature increase of B is nonzero and increasing for lower values of the damping. Unexpectedly, at the smallest value for the damping considered ($\alpha_\perp = 0.001$), the nonswitching small
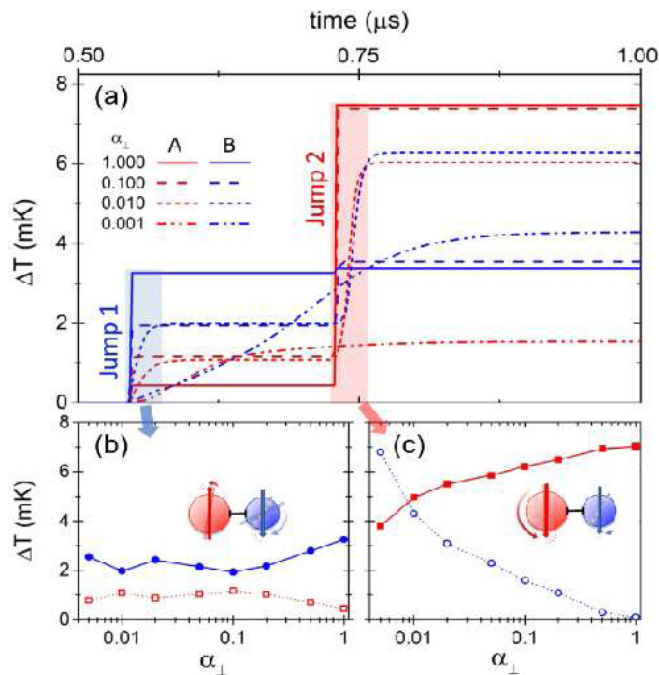
FIG. 5. (a) Temperature dynamics of both nanoparticles A (red) and B (blue) for four values of the damping parameter. The temperature changes of particles A and B as a function of $\alpha_\perp$ at jumps 1 and 2 are shown in (b) and (c), respectively. Again, the nanoparticles are separated by $x = 7.1$ nm.

nanoparticle B releases more energy during jump 2 than the switching one A. The change in interaction energy goes into precession (work) and into heat in a way which is not easy to predict. Since realistic nanoparticles have small damping parameters, the above scenario makes it impossible to evaluate the heat from individual hysteresis loops or considerations of internal energy changes. Our dynamical approach, on the other hand, distinguishes between the local heat released by each nanoparticle and the amount of energy which goes into interactions.

III. CONCLUSIONS

In conclusion, we have shown that interacting magnetic nanoparticles exhibit a complex scenario of local heat transfer, since the particles do work on each other as well as having work done on them by an applied external field, and this work is highly path dependent. Of particular note, interacting nanoparticles produce heat not only when their magnetization irreversibly switches between two energy wells, but also when experiencing intrawell magnetization dynamics. In other words, when one particle switches, another necessarily has a changed dipolar field and its magnetization therefore has

work done on it which can be converted to heat. The released heat depends nontrivially on the coupling to the bath, i.e., on the damping parameter $\alpha_\perp$, since this alters the dynamical magnetization path and therefore the work. This complexity does not allow a simple interpretation of the produced heat in terms of the local hysteresis loops. When the strength of interactions increases, local loops may become negative, corresponding to the fact that a large part of the energy transferred is work done on/by another particle and only part of it is released into the environment as heat. Furthermore, our results highlight the fact that heating occurs at a much faster timescale than the field frequency (at the nanosecond timescale of magnetization reversal).

It is important to reiterate that the work presented here is not statistical in nature, in contrast to most models that estimate the energy dissipated in magnetic nanoparticle systems. Once the dissipated energy is estimated for an ensemble of particles, researchers then need to predict how that heat is transported away from particles, typically using the so-called bioheat equation [3,29]. This is still the case for our model of individual particles and is beyond the scope of this article. However, note that the big advantage here is to predict *which* particle is producing heat, in which amount, and over which timescales. Recent experiments point to the fact that this local heat production is more important than the global temperature change [6–8].

Our method opens the possibility to evaluate local heat dissipation by nanoparticles in complex scenarios, such as in *in vivo* aggregates, as a function of distance and time. Our results strengthen the understanding of magnetic hyperthermia and will allow optimization of magnetic nanoparticles for its improved performance. Our results also address the understanding of intrinsic entanglement of heat and magnetization dynamics. The proposed method can serve as theoretical background in many other magneto-thermodynamical applications where spin and temperature dynamics and coupled, such as magnetocaloric and magnetic refrigeration applications, all-optical magnetization switching or spintronics based on the spin-Seebeck, spin-Peltier, or Nernst effects.

[1] T. K. Houlding and E. V. Rebrov, Application of alternative energy forms in catalytic reactor engineering, Green Process. Synth. **1**, 19 (2012).

[2] M. M. Beck, C. Lammel, and B. Gleich, Improving heat generation of magnetic nanoparticles by pre-orientation of particles in a static three tesla magnetic field, J. Magn. Magn. Mater. **427**, 195 (2017).

[3] E. A. Périgo, G. Hemery, O. Sandre, D. Ortega, E. Garaio, F. Plazaola, and F. J. Teran, Fundamentals and advances in magnetic hyperthermia, Appl. Phys. Rev. **2**, 041302 (2015).

[4] MagForce Nanotechnologies AG, Berlin, Germany, http://www.magforce.de/en/home.html (2016).

[5] X. Liu, Y. Zhang, Y. Wang, W. Zhu, G. Li, X. Ma, Y. Zhang, S. Chen, S. Tiwari, K. Shi, S. Zhang, H. M. Fan, Y. X. Zhao, and X.-J. Liang, Comprehensive understanding of magnetic hyperthermia for improving antitumor therapeutic efficacy, Theranostics **10**, 3793 (2020).

[6] E. Cazares-Cortes, S. Cabana, C. Boitard, E. Nehlig, N. Griffete, J. Fresnais, C. Wilhelm, A. Abou-Hassan, and C. Menager, Recent insights in magnetic hyperthermia: From the "hot-spot" effect for local delivery to combined magneto-photo-thermia using magneto-plasmonic hybrids, Adv. Drug Delivery Rev. **138**, 233 (2019).

[7] A. Riedinger, P. Guardia, A. Curcio, M. A. Garcia, R. Cingolani, L. Manna, and T. Pellegrino, Subnanometer local temperature probing and remotely controlled drug release based on azo-functionalized iron oxide nanoparticles, Nano Lett. **13**, 2399 (2013).

[8] J. T. Dias, M. Moros, P. del Pino, S. Rivera, V. Grazú, and J. M. de la Fuente, DNA as a molecular local thermal probe for the analysis of magnetic hyperthermia, Angew. Chem. Int. Ed. **52**, 11526 (2013).

[9] M. Creixell, A. C. Bohórquez, M. Torres-Lugo, and C. Rinaldi, Egfr-targeted magnetic nanoparticle heaters kill cancer cells without a perceptible temperature rise, ACS Nano **5**, 7124 (2011).

[10] A. Villanueva, P. de la Presa, J. M. Alonso, T. Rueda, A. Martínez, P. Crespo, M. P. Morales, M. A. Gonzalez-Fernandez, J. Valdés, and G. Rivero, Hyperthermia HeLa cell treatment with silica-coated manganese oxide nanoparticles, J. Phys. Chem. C **114**, 1976 (2010).

[11] D. Cabrera, A. Coene, J. Leliaert, E. J. Artés-Ibáñez, L. Dupré, N. D. Telling, and F. J. Teran, Dynamical magnetic response of iron oxide nanoparticles inside live cells, ACS Nano **12**, 2741 (2018).

[12] I. Castellanos-Rubio, I. Rodrigo, A. Olazagoitia-Garmendia, O. Arriortua, I. Gil de Muro, J. S. Garitaonandia, J. R. Bilbao, M. L. Fdez-Gubieda, F. Plazaola, I. Orue, A. Castellanos-Rubio, and M. Insausti, Highly reproducible hyperthermia response in water, agar and cellular environment by discretely pegylated magnetite nanoparticles, ACS Appl. Mater. Interfaces **12**, 27917 (2020).

[13] M. L. Etheridge, K. R. Hurley, J. Zhang, S. Jeon, H. L. Ring, C. Hogan, C. L. Haynes, M. Garwood, and J. C. Bischof, Accounting for biological aggregation in heating and imaging of magnetic nanoparticles, TECHNOLOGY **02**, 214 (2014).

[14] I. Conde-Leboran, D. Baldomir, C. Martinez-Boubeta, O. Chubykalo-Fesenko, M. P. Morales, G. Salas, D. Cabrera, J. Camarero, F. J. Teran, and D. Serantes, A single picture explains diversity of hyperthermia response of magnetic nanoparticles, J. Phys. Chem. C **119**, 15698 (2015).

[15] R. E. Rosensweig, Heating magnetic fluid with alternating magnetic field, J. Magn. Magn. Mater. **252**, 370 (2002).

[16] R. P. Tan, J. Carrey, and M. Respaud, Magnetic hyperthermia properties of nanoparticles inside lysosomes using kinetic Monte Carlo simulations: Influence of key parameters and dipolar interactions, and evidence for strong spatial variation of heating power, Phys. Rev. B **90**, 214421 (2014).

[17] S. Ruta, R. Chantrell, and O. Hovorka, Unified model of hyperthermia via hysteresis heating in systems of interacting magnetic nanoparticles, Sci. Rep. **5**, 9090 (2015).

[18] O. Hovorka, J. Barker, G. Friedman, and R. W. Chantrell, Role of geometrical symmetry in thermally activated processes in clusters of interacting dipolar moments, Phys. Rev. B **89**, 104410 (2014).

[19] P. Torche, C. Munoz-Menendez, D. Serantes, D. Baldomir, K. L. Livesey, O. Chubykalo-Fesenko, S. Ruta, R. Chantrell, and O. Hovorka, Thermodynamics of interacting magnetic nanoparticles, Phys. Rev. B **101**, 224429 (2020).

[20] Y. P. Kalmykov, S. V. Titov, D. J. Byrne, W. T. Coffey, M. Zarifakis, and M. H. Al Bayyari, Dipole-dipole and exchange interaction effects on the magnetization relaxation of two macrospins: Compared, J. Magn. Magn. Mater. **507**, 166814 (2020).

[21] W. Coffey, Y. Kalmykov, and S. Titov, *Thermal Fluctuations and Relaxation Processes in Nanomagnets* (Word Scientific, Singapore, 2020).

[22] C. Munoz-Menendez, I. Conde-Leboran, D. Baldomir, O. Chubykalo-Fesenko, and D. Serantes, The role of size polydispersity in magnetic fluid hyperthermia: Average vs. local infra/over-heating effects, Phys. Chem. Chem. Phys. **17**, 27812 (2015).

[23] P. Nieves, D. Serantes, and O. Chubykalo-Fesenko, Self-consistent description of spin-phonon dynamics in ferromagnets, Phys. Rev. B **94**, 014409 (2016).

[24] J. Y. Yang, J. H. Kim, J. S. Lee, S. J. Woo, J. S. Kwak, J. P. Hong, and M. H. Jung, Inverted hysteresis loops observed in a randomly distributed cobalt nanoparticle system, Phys. Rev. B **78**, 094415 (2008).

[25] S. Gu, W. He, M. Zhang, T. Zhuang, Y. Jin, H. El Bidweihy, Y. Mao, J. H. Dickerson, M. J. Wagner, E. Della Torre, and L. H. Bennett, Physical justification for negative remanent magnetization in homogeneous nanoparticles, Sci. Rep. **4**, 6267 (2014).

[26] M. Madami, G. Gubbiotti, S. Tacchi, and G. Carlotti, Magnetization dynamics of single-domain nanodots and minimum energy dissipation during either irreversible or reversible switching, J. Phys. D: Appl. Phys. **50**, 453002 (2017).

[27] R. Otxoa, U. Atxitia, P. Roy, and O. Chubykalo-Fesenko, Giant localised spin-Peltier effect due to ultrafast domain wall motion in antiferromagnetic metals, Commun. Phys. **3**, 31 (2020).

[28] W. T. Coffey, D. S. F. Crothers, J. L. Dormann, Y. P. Kalmykov, E. C. Kennedy, and W. Wernsdorfer, Thermally Activated Relaxation Time of a Single Domain Ferromagnetic Particle Subjected to a Uniform Field at an Oblique Angle to the Easy Axis: Comparison with Experimental Observations, Phys. Rev. Lett. **80**, 5655 (1998).

[29] K.-H. Chen, B.-C. Chen, and C.-Y. Ho, Hyperthermia temperature of magnetic fluid with superparamagnetic nanoparticles subjected to an alternating magnetic field, J. Nanosci. Nanotechnol. **18**, 3018 (2018).